


Article

# Simplified Strength Assessment for Preliminary Structural Design of Floating Offshore Wind Turbine Semi-Submersible Platform

Yan Dong <sup>1,2,3</sup>, Jian Zhang <sup>1</sup>, Shaofeng Zhong <sup>1</sup> and Yordan Garbatov <sup>3,4,\*</sup> 

<sup>1</sup> Yantai Research Institute of Harbin Engineering University, Harbin Engineering University, Yantai 264006, China; yan.dong@hrbeu.edu.cn (Y.D.); 15763602790@163.com (J.Z.); zhong\_s\_f@163.com (S.Z.)

<sup>2</sup> College of Shipbuilding Engineering, Harbin Engineering University, Harbin 150001, China

<sup>3</sup> HEU-UL International Joint Laboratory of Naval Architecture and Offshore Technology, Harbin 150001, China

<sup>4</sup> Centre for Marine Technology and Ocean Engineering (CENTEC), Instituto Superior Técnico, Universidade de Lisboa, 1049-001 Lisbon, Portugal

\* Correspondence: yordan.garbatov@tecnico.ulisboa.pt

**Abstract:** The study aims to develop a simplified strength assessment method for the preliminary structural design of a semi-submersible floating offshore wind turbine platform. The method includes load cases with extreme wave load effects and a load case dominated by wind load. The extreme load effects due to waves are achieved using the design waves. Seven characteristic responses of the semi-submersible platform due to waves are chosen. The design waves for the extreme characteristic responses are all from extreme wave conditions where the significant wave heights are close to the one for a return period of 100 years. The extreme load effects dominated by wind loads are approximated using the modified environmental contour method. The load effects are the tower base shear force and bending moment. The two load effects are correlated, and a linear equation can approximate the relationship between their extreme values. The finite element analysis results show that the frame design of the bottom of the outer column is essential for structural strength. The wave load can also result in significant stress in the area close to the tower base.



**Citation:** Dong, Y.; Zhang, J.; Zhong, S.; Garbatov, Y. Simplified Strength Assessment for Preliminary Structural Design of Floating Offshore Wind Turbine Semi-Submersible Platform. *J. Mar. Sci. Eng.* **2024**, *12*, 259. <https://doi.org/10.3390/jmse12020259>

Academic Editor: Constantine Michailides

Received: 1 January 2024

Revised: 27 January 2024

Accepted: 30 January 2024

Published: 31 January 2024



**Copyright:** © 2024 by the authors. Licensee MDPI, Basel, Switzerland. This article is an open access article distributed under the terms and conditions of the Creative Commons Attribution (CC BY) license (<https://creativecommons.org/licenses/by/4.0/>).

**Keywords:** floating offshore wind turbine; design load; environmental contour; design wave method

## 1. Introduction

Floating offshore wind turbines (FOWTs) have gained significant attention in recent years because they have the potential to harvest a considerable amount of clean energy. Although some FOWTs have been in service, substantial efforts are still needed to have a cost-effective structural design that can satisfy safety requirements and have relatively low capital expenditure.

The structural design of an FOWT is generally performed according to standards, e.g., IEC 61400-3 [1] and DNV-ST-0119 [2]. The integrated system simulation should be carried out in the time domain to evaluate the motions and loads. The structural safety of an FOWT design is verified under fatigue and extreme loads. Many design load cases (DLCs) are specified by the standard, covering the most significant conditions an FOWT may experience during its lifetime.

One challenge for the structure design lies in the structural load effect analysis of the support structure because the support structure is usually treated as a rigid body in the time-domain simulation [3]. Many studies have focused on the dynamic load or load effects of specific locations such as the blade, tower base, mooring line, etc. [4–8]. A limited number of studies concentrated on the structural load effect analysis of the support structure, which is essential for structural design. Wang et al. [3] employed a novel methodology using the SESAM package to obtain the time-domain cross-sectional forces and moments of a semi-submersible hull of a 10 MW FOWT accounting for the static and dynamic global

loads under the still water, wind, and wave loads and associated motions. Luan et al. [9] developed and verified a time-domain multibody approach for determining global forces and moments in the structural components of FOWTs. Wang and Moan [10,11] outlined a practical multibody approach and procedure to determine load effects for the structural design of semi-submersible hulls. They applied column design and extreme internal load effect analysis.

Another limitation of the design process specified by the standard is the large number of simulations. It has been shown by Park and Choung [12] that (only for DLC 6.2 specified in IEC 61400-3 [1]), the number of sub DLCs can be up to 5832, not to mention that at least 6 h of simulation is needed for each case. Covering all the DLCs in the preliminary design stage is complex, and only some representative load cases have been assessed in many previous studies. Park and Choung [12] generated several direct strength analysis cases combining the long-term acceleration and nacelle thrust to maximise the forces in the surge, sway, and heave directions. Zavvar et al. [13] conducted a preliminary structural design considering the still water and above-rated conditions. Wang and Moan [10,11] determined extreme stresses on semi-submersible hulls of floating wind turbines based on the load cases corresponding to significant wind speeds and critical wave periods on the environmental contour.

The design wave method widely used to calculate wave-induced load effects of ships and offshore structures is based on frequency domain analysis, which cannot correctly deal with nonlinearities, transient effects, and wind load effects of FOWTs. However, the traditional method may still be used if the wave load dominates the load effects. Zhang et al. [14] have shown that for the accelerations in three directions of an FOWT semi-submersible platform, the extreme values determined by the design wave method are more significant than those specified by fully coupled time-domain simulations. In wave load-dominated cases, the extreme load effects are associated with extreme wave conditions. The extreme wave conditions and the extreme wind speeds generally happen simultaneously. The wind load in extreme wind speed is less significant than in rated wind speed. That may be the reason that the design wave method is still applicable. For the load effects dominated by the wind load, e.g., the tower base forces and moments, the time domain approach based on the modified environmental contour method [15] may be used to approximate the long-term extremes of the load effect for the strength assessment.

The present study aims to propose a simplified strength assessment method for the preliminary structural design of an FOWT support structure to avoid the difficulty in the load effect analyses and the significant number of time-domain simulations. The procedure consists of some load cases with extreme wave load effects and a load case dominated by the wind load. The NREL 5-MW wind turbine and the OC4 semi-submersible platform developed for the DeepCwind project are used. The wind and wave are considered uni-directional, which is believed to be conservative in most cases [16].

## 2. Methodology

### 2.1. Stochastic Design Wave Method

It is a common practice to use the design wave method to evaluate the global strength of ship and offshore structures [17,18]. The design wave is the regular wave that gives the same level as the long-term design value for a characteristic response. The long-term design value is to be determined for a specific site at a return period of 100 years. The stochastic design wave methods are employed in the present study.

The stochastic design wave method determines the design wave amplitude by the extreme value of the short-term prediction of the characteristic response. The irregularity of the wave is considered by the method. The procedure of the method can be described as follows.

1. Determine the critical wave heading and length (or critical wave period) and calculate the RAOs, the same as the deterministic design wave method.

2. Calculate the design significant wave heights based on the irregular sea steepness for a range of average zero up-crossing wave periods.
3. Derive the wave energy spectrum,  $S_w(\omega)$  for each irregular sea state found in step (2) as a function of significant wave height,  $H_s$ , and average zero up-crossing wave period,  $T_z$ . An appropriate wave energy spectrum, e.g., Pierson–Moskovitz (P-M) or JONSWAP, should be selected.

4. Calculate the response spectrum,  $S_R(\omega)$  based on the RAO and the wave energy spectrum:

$$S_R(\omega) = [RAO(\omega)]^2 S_w(\omega) \tag{1}$$

5. Predict the maximum response  $R_{max}$  for each irregular sea state found in step (2) as follows:

$$R_{max} = \sqrt{m_0} \sqrt{2 \ln N} \tag{2}$$

where  $m_0$  is the area of the response spectrum,  $N$  is the number of response cycles, which equals  $D/T_a$  the duration of the short-term sea state,  $T_a$  is the average response zero up-crossing period  $2\pi\sqrt{m_0/m_2}$  and  $m_2$  is the second moment of the spectrum.

6. Select the maximum response among the irregular sea states considered, and calculate the design regular wave amplitude,  $A_D$ , as follows:

$$A_D = \frac{R_{max}}{RAO_c} LF \tag{3}$$

where  $RAO_c$  is the peak RAO at the critical wave period, and  $LF$  is the load factor ranging from 1.1 to 1.3.

The irregular sea steepness  $S_S$  is defined as:

$$S_S = \frac{2\pi H_s}{g T_z^2} \tag{4}$$

The significant wave height is less than the maximum significant wave height at a return period of 100 years,  $H_{s100}$ . In addition, the irregular sea steepness need not be taken greater than [17]:

$$S_S = \begin{cases} 1/10 & T_z \leq 6 \text{ s} \\ 1/15 & T_z \geq 12 \text{ s} \\ \text{Linear interpolation for} & 6 \text{ s} < T_z < 12 \text{ s} \end{cases} \tag{5}$$

Therefore, by combining Equations (4) and (5), the limiting  $H_s$  as a function of  $T_z$  can be obtained, which indicates the design sea state to be evaluated.

### 2.2. Modified Environmental Contour Method

To predict the extreme response, the Full Long-Term Analysis (FLTA) is straightforward and considers all the combinations of the essential environmental parameters. The long-term extreme cumulative distribution function (CDF) can be calculated by integrating all the environmental parameters and the corresponding short-term extreme CDF [15]:

$$F_X^{LT}(\xi) = \int F_{X|S}^{ST}(\xi|s) f_S(s) ds \tag{6}$$

where  $\xi$  is the extreme value of the response of  $X$  in a period,  $s$  is a set of environmental parameters representing the short-term environmental condition,  $f_S(s)$  is the probability density function (PDF) of  $s$ ,  $F_X^{LT}(\xi)$  and  $F_{X|S}^{ST}(\xi)$  are the long-term and short-term CDF of  $\xi$ , respectively. The mean wind speed,  $U_w$ , significant wave height,  $H_s$ , and spectral peak period,  $T_p$ , are the dominant environmental parameters for FOWTs. If the time of the short-term condition is 1 h, which is used in the present study, the  $N$ -year extreme value

may be found by  $1 - F_X^{LT}(\xi) = 1 / (N \times 365.25 \times 24)$ . FLTA is time-consuming because it requires many simulations to cover all the environmental conditions.

Simplified methods have been developed to improve efficiency. The first order reliability method (FORM) uses a tangent hyperplane to approximate the limit state surface at the design point in standard normalised random space, known as U-space. The limit state surface collects all the conditions that result in the same response. The design point is located on the limit state surface and closest to the origin in the U-space. The distance between the design point and the origin can approximate the failure probability. The  $N$ -year extreme response corresponding to a certain exceedance probability has to be found by iterations if the FORM is used. The Inverse first order reliability method (IFORM) can provide a more efficient way to obtain the long-term extreme response corresponding to a target return period. The IFORM creates a hypersphere with a radius related to the target exceedance probability in the U-space and transforms it to the original physical space by Rosenblatt transformation [19]. A point on the hypersphere, where the response attains its maximum value, is identified. The maximum value approximates the  $N$ -year extreme response.

The environmental contour method (ECM) [20,21] is a further simplification of the IFORM, and is incorporated in the standard IEC 61400-3 [1]. The variability of the short-term extreme response is ignored, and only environmental parameters are involved in the contour. The ECM selects important environmental conditions on the contour surface with a specific target return period. In the U-space, the contour surface of the  $N$ -year return period is a hypersphere with radius  $r$ :

$$r = \Phi^{-1} \left( 1 - \frac{1}{N \times 365.25 \times 24} \right) \tag{7}$$

where  $\Phi$  is CDF of the standard normal distribution, the environmental condition with the most significant extreme response, which approximates well the long-term extreme responses, is chosen. The variability of the short-term extreme response is important for many marine structures. Ignoring the variability of the short-term extreme response generally underestimates the long-term extreme responses [22]. Stochastic simulations are performed for each environmental condition. An empirical fractile, typically ranging from 85% to 95%, of short-term extreme response probability distribution can be applied to compensate for the underestimation [21].

It has been shown in some studies that the ECM does not perform well for offshore wind turbines due to the non-monotonic behaviour of the wind load [23]. The wind load typically reaches the maximum value at the rated wind speed, decreases with a further increase in the wind speed, and drops rapidly at the cut-out wind speed. Li et al. [15] proposed a modified ECM to identify the most critical environmental condition governing the long-term extreme for the dominant responses by wind. The idea of the modified ECM is to extrapolate the short-term extreme for the return period of  $N$ -year to the 50-year extreme, where  $N$  is chosen such that ECM can perform well:

$$F_{x,50}(\xi) = \left[ F_{X|U_w, H_s, T_p}^{ST}(\xi | u_N, h_N, t_N) \right]^{50/N} \tag{8}$$

where  $(u_N, h_N, t_N)$  is the environmental condition on the  $N$ -year environmental contour. The procedure of the modified ECM is shown in Figure 1 when considering combined wind and wave loads. Multiple contours within the operational wind speed range are checked. The most probable value of the extrapolated extreme distribution.

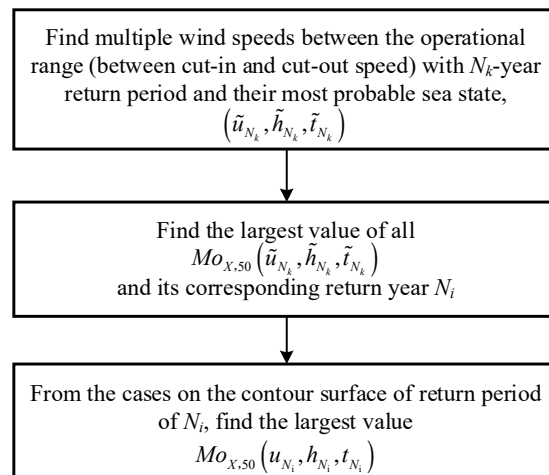


Figure 1. Procedure of modified ECM [15].

For each environmental condition to be evaluated, many simulations are required to obtain the short-term 1 h extreme probability distribution. In the present study, 1 h extremes are extrapolated from 10 min extremes. It is assumed that the 10 min extreme follows the Gumbel distribution:

$$F_{X_{10\text{-min}}}(\xi) = e^{-e^{-\frac{\xi-\mu}{\beta}}} \tag{9}$$

where  $\mu$  and  $\beta$  are the distribution parameters and the above equation can be rewritten as a linear equation:

$$\xi = \beta[-\ln(-\ln F_{X_{10\text{-min}}})] + \mu \tag{10}$$

The two distribution parameters can be estimated by the least square method for linear regression based on n data points obtained from n times simulation. Since there are six 10 min periods in 1 h, assuming independence, the 1 h extreme CDF,  $F_{X_{1\text{-h}}}$  can be calculated based on the 10 min CDF,  $F_{X_{10\text{-min}}}$  by:

$$F_{X_{1\text{-h}}}(\xi) = [F_{X_{10\text{-min}}}(\xi)]^6 \tag{11}$$

The extrapolation of 50-year 1 h CDF is described by:

$$F_{X_{1\text{-h},50}}(\xi) = [F_{X_{10\text{-min}}^{ST}|U_w,H_s,T_p}(\xi|u_{N_i}, h_{N_i}, t_{N_i})]^{6 \times 50 / N_i} \tag{12}$$

The most probable value can be obtained by:

$$Mo_{X_{1\text{-h},50}}(u_{N_i}, h_{N_i}, t_{N_i}) = \mu + \beta \ln\left(\frac{6 \times 50}{N_i}\right) \tag{13}$$

To check whether the number of simulations, n, is enough, the 95% confidence interval (CI) of  $Mo_{X_{1\text{-h}}}$  is obtained using the method described in [15]. The ratio between the 95% CI and the value obtained using Equation (13) is computed. If the ratio is above 3%, more simulations are needed.

### 2.3. Load Cases for the Simplified Strength Assessment Method

The load cases used for the preliminary strength assessment are proposed in this section. It has been shown in Section 2.1 that the design waves are obtained based on a return period of 100 years and a load factor ranging from 1.1 to 1.3. For FOWTs, the return period for the extreme design load estimation is 50 years [1]. Therefore, if FOWTs are only subjected to the wave load effects, the design wave method is more conservative than the

method based on the standards for FOWTs. Therefore, the design wave method may still be reasonable if the wave load effects dominate. The wave design method cannot correctly consider the nonlinearities, transient effects, and wind load effects. These effects can be covered by the overestimated wave load effects when using the design wave method.

According to the features of the OC4 semi-submersible platform, the following characteristic responses are chosen, whose extremes are achieved using design waves (see Figure 2). They are the accelerations in three directions ( $a_x$ ,  $a_y$ , and  $a_z$ ), the split force between two outer columns ( $F_T$ ), the split force between one outer column and the other two outer columns ( $F_L$ ), the shear force between one outer column and the other two columns ( $F_S$ ), and the torsion moment between one outer column and the other two columns ( $M_L$ ). The vertical bending moments are less likely to develop significantly because the semi-submersible platform is not as long as ships. Therefore, the vertical bending moment is not considered in the present study.

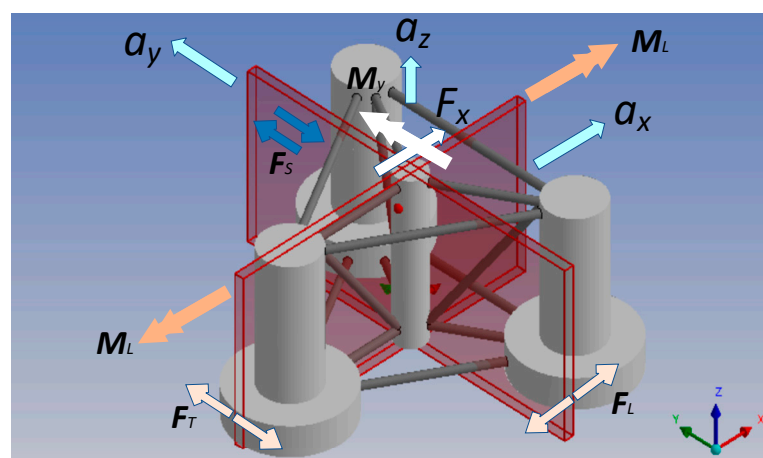


**Figure 2.** Characteristic responses of the OC4 semi-submersible platform under wave load.

For the load effects that are dominated by the wind load, the extreme load effects are estimated based on the modified ECM. In the present study, the extreme tower base shear force,  $F_x$ , and bending moment,  $M_y$ , are obtained and applied to the finite element model for structural strength assessment. The load cases for the simplified strength assessment method are summarised in Table 1.

**Table 1.** Load cases for the simplified strength assessment method.

Load Case	Extreme Load Effects	Method
1	$a_x$	Stochastic design wave method
2	$a_y$	Stochastic design wave method
3	$a_z$	Stochastic design wave method
4	$F_T$	Stochastic design wave method
5	$F_L$	Stochastic design wave method
6	$F_S$	Stochastic design wave method
7	$M_L$	Stochastic design wave method
8	$F_x, M_y$	Modified ECM

The load cases are developed for the specific FOWT support structure. The proposed method may be used in the preliminary design of similar FOWT support structures, in which the load cases can be altered based on the characteristics of the support structure.

### 3. Numerical Model Description and Environment

#### 3.1. Numerical Model

The OC4 semi-submersible platform has a centre column connected to the tower and three outer columns. The centre column and outer column are connected using pontoons and braces. The bottom of the outer column has a larger diameter to suppress motion. The main dimensions of the platform can be found in [24].

Because the structural components of the platform, e.g., the plate thickness, the dimension of the stiffener, etc., whose strength will be checked, are preliminarily determined according to the classification society rule, the resulting total metal mass is different from those in [24]. The ballast in the columns is adjusted to guarantee the whole mass, and the centre of mass is similar to the original ones. The floating platform structural properties used in the present study are listed in Table 2.

**Table 2.** Floating platform structural properties.

Structural Property	Value
Weight of displaced fluid	$1.42 \times 10^7$ kg
The centre of mass below SWL	13.487 m
Draft	20 m
Radius of gyration $K_{xx}$	20.99 m
Radius of gyration $K_{yy}$	20.99 m
Radius of gyration $K_{zz}$	27.16 m
Mass of ballast in outer column	$2.93 \times 10^6$ kg
Mass of ballast in centre column	$1.47 \times 10^6$ kg

The hydrodynamic analyses are carried out using ANSYS AQWA 2021 R1. Panels model the columns, and Morison elements model the connections between the columns. The hydrodynamic models and the coordinates are shown in Figure 3. The mesh convergence is checked before the model is applied. The size of the panels is 1.2 m, and the size of the Morison elements is 1.2 m. The numerical model is validated by comparing it with the results of an existing numerical study. The heave and pitch RAOs predicted by the present study and Zhu [25] are shown in Figure 4. Good agreement is achieved, indicating that the hydrodynamic analysis model is reliable.

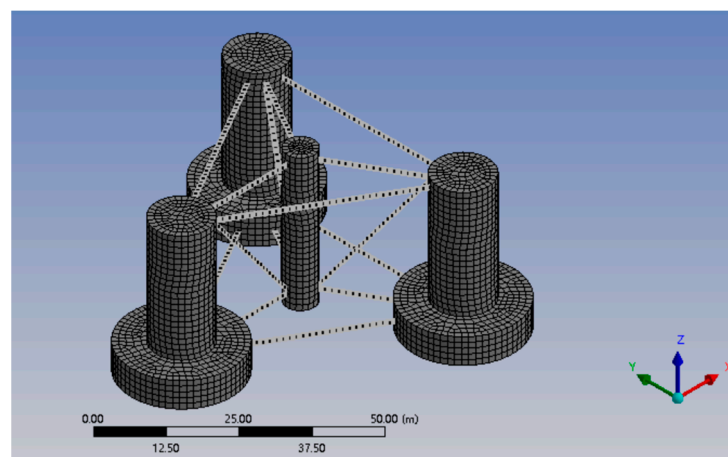


**Figure 3.** Hydrodynamic model in ANSYS AQWA.

The results may be overestimated because the potential theory cannot consider viscous damping. Equivalent viscous damping, which is proportional to critical damping, is used in the present study to improve accuracy. Viscous damping of rolling, pitching, and heaving are considered. A 5% critical damping is employed for the RAO calculation.

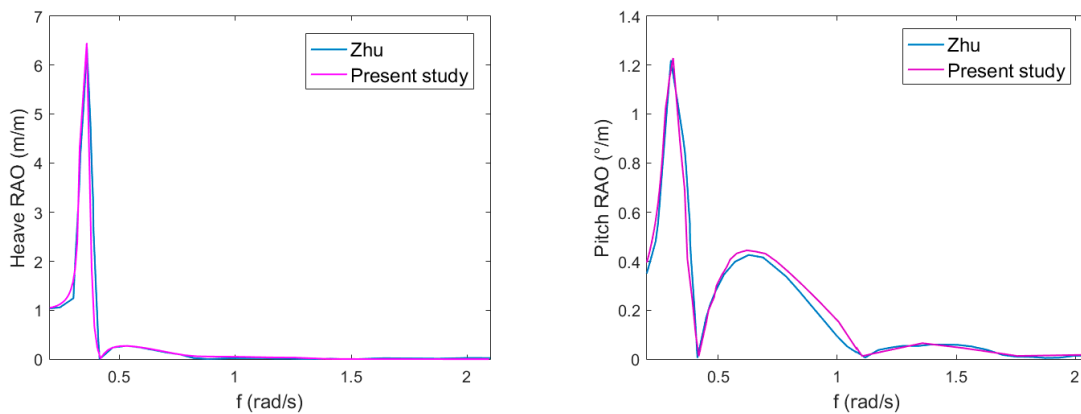


Figure 4. Heave and pitch RAOs predicted by the present study and Zhu [25].

The structural components of the semi-submersible platform are shown in Figure 5. The finite element model of the semi-submersible platform is constructed in ANSYS Workbench 2021 R1. The mesh condition of the outer column is also shown in the figure. The finite element model consists of shell elements and beam elements. The outer surfaces of the columns, bulkheads, braces, and strong frames are modelled by shell elements. Circumferential and vertical beams stiffen the four columns. Each outer column is divided by several horizontal bulkheads, stiffened by beams. Strong frames support the bottom of the outer column. The shell element models the tower, and the nacelle, rotor, and blades are modelled as mass elements. The mesh size of the structural model is about 0.2 m. The mesh size is smaller than the one usually used in the global analyses of ships and offshore structures, which is the stiffener spacing for the coarse mesh model.

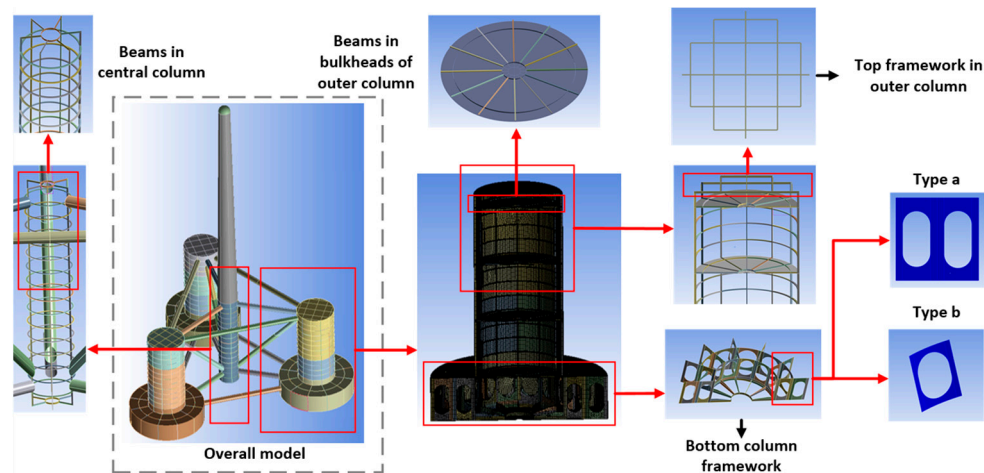
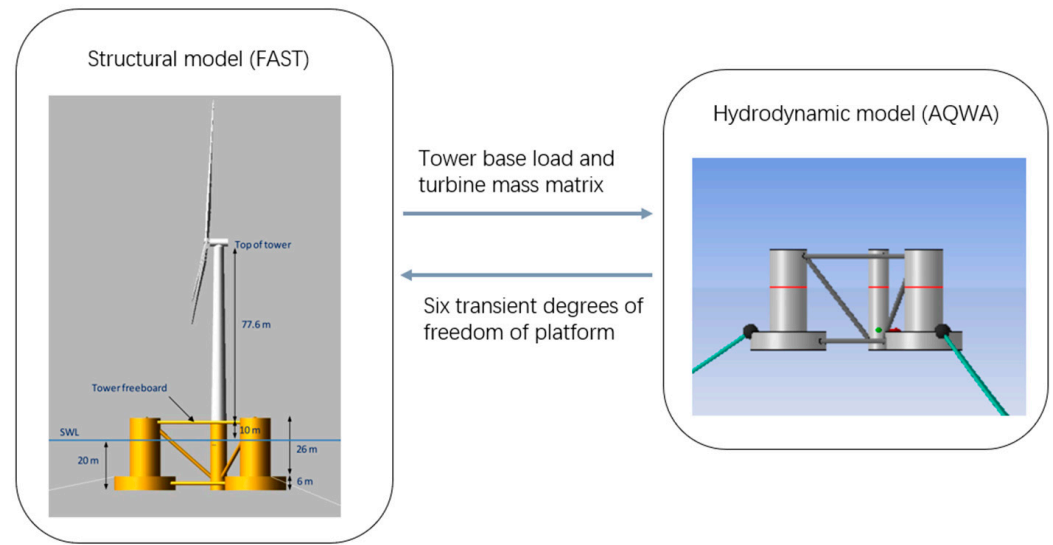


Figure 5. Structural model of the semi-submersible platform for the FOWT.

The coupling framework based on FAST and ANSYS AQWA, denoted as F2A, for dynamic analysis of FOWTs developed by Yang et al. [26] is used in the time-domain simulation. The coupling is achieved by modifying the source codes of FAST and the dynamic link library (DLL) of AQWA. The coupling framework has been validated by comparing it with OpenFAST, and some advantages of the coupling framework have been noticed [26]. The floating offshore wind turbine model in a time-domain simulation is shown in Figure 6. The dynamic model of the turbine coupling system is established based on FAST, and the hydrodynamic model is calculated by combining potential flow theory with the Morison equation. The NREL 5-MW reference wind turbine is used in the simulation, and the mooring system is the same as those introduced in [24]. The Kaimal wind and the P-M wave spectra are chosen in the simulation. The turbulent intensity is 12%. The time step of the wind turbine dynamic simulation is 0.005 s, and the time step of



the hydrodynamic simulation is 0.1 s. For each simulation, the analysis time is 800 s with a transient start-up time of 200 s.



**Figure 6.** Time-domain coupling process of FAST and ANSYS AQWA.

The results from F2A are compared with those from OpenFAST 3.1.0 to validate the numerical method. The comparison was also carried out by Yang et al. [26] to validate the framework. The thrust force under turbulent wind with a mean wind speed of 11.4 m/s at the hub, and the heave motion of the platform under regular wave height of 4 m and wave period of 18 s are shown in Figure 7. Good agreement is achieved, indicating that F2A is also a reliable tool for coupling analyses of FOWTs.

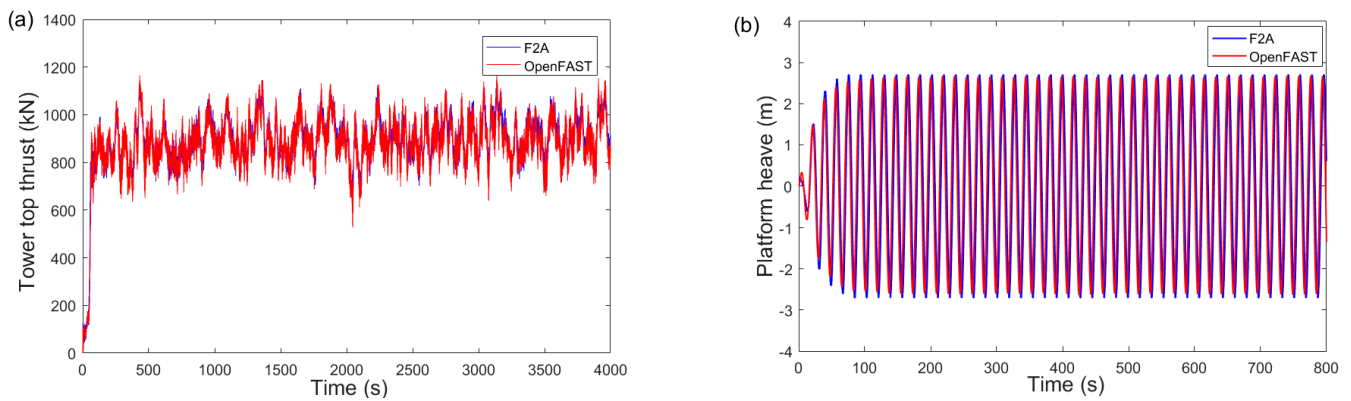


**Figure 7.** Thrust force (a) and Heave motion (b) between the F2A and OpenFAST.

The design wave parameters are determined based on hydrodynamic analyses for the load cases based on design waves. The loads and motions caused by the design waves are obtained using ANSYS AQWA and applied to the finite element model in ANSYS Workbench. The time-domain simulations are carried out using the coupling framework based on FAST and AQWA for the load cases dominated by wind loads. The estimated extreme tower base shear force and bending moment are applied to the finite element model. The inertia relief technique is used in the finite element analysis.

### 3.2. Metocean Information

The environment of the Norway 5 site (site 14 in [27]) is employed in the present study. One-hour joint environmental statistics of  $U_w$  (10 m above the mean sea level),  $H_s$ , and  $T_p$  were obtained by Li et al. [27]. The joint distribution is:

$$f_{U_w, H_s, T_p}(u, h, t) = f_{U_w}(u) f_{H_s|U_w}(h|u) f_{T_p|U_w, H_s}(t|u, h) \tag{14}$$

The wind speed follows the Weibull distribution:

$$F_{U_w}(u) = 1 - \exp\left[-\left(\frac{u}{\beta_u}\right)^{\alpha_u}\right] \tag{15}$$

The conditional significant wave height also follows the Weibull distribution:

$$F_{H_s|U_w}(h|u) = 1 - \exp\left[-\left(\frac{h}{\beta_h(u)}\right)^{\alpha_h(u)}\right] \tag{16}$$

where

$$\alpha_h(u) = a_1 + a_2 u^{a_3}, \beta_h(u) = b_1 + b_2 u^{b_3} \tag{17}$$

The spectral peak period conforms to the log-normal distribution, given a combination of  $U_w$  and  $H_s$ :

$$f_{T_p|U_w, H_s}(t|u, h) = \frac{1}{2\pi\sigma_{\ln(T)}t} \exp\left[-\frac{1}{2}\left(\frac{\ln(t) - \mu_{\ln(T)}}{\sigma_{\ln(T)}}\right)^2\right] \tag{18}$$

where

$$\mu_{\ln(T)} = \ln\left(\frac{\mu_T}{\sqrt{1 + \nu_T^2}}\right), \sigma_{\ln(T)} = \sqrt{\ln(1 + \nu_T^2)} \tag{19}$$

$$\mu_T = \bar{t}(h) \left[1 + \theta\left(\frac{u - \bar{u}(h)}{\bar{u}(h)}\right)^\gamma\right], \nu_T = k_1 + k_2 e^{hk_3} \tag{20}$$

$$\bar{t}(h) = e_1 + e_2 h^{e_3}, \bar{u}(h) = f_1 + f_2 h^{f_3} \tag{21}$$

The parameters involved in the distribution models can be found in [27].

The wind speeds at different heights can be calculated using a power-law wind shear profile:

$$V(z) = U_w \left(\frac{z}{10}\right)^{0.1} \tag{22}$$

Because the maximum significant wave height and regular wave height at a return period of 100 years are required in the design wave method, they are estimated using the above environmental statistics. The marginal distribution of  $H_s$  is obtained and  $H_{s100}$  is determined based on the exceedance probability of  $1/(100 \times 365.25 \times 24)$ . The estimation results are  $H_{s100} = 14.15$  m.

## 4. Results

### 4.1. Design Waves

The  $RAO_S$  are shown in Figure 8. For the vertical acceleration  $RAO_S$ , the wave angles from  $0^\circ$  to  $60^\circ$  with an interval of  $15^\circ$  are considered due to the triangular shape of the platform. For the other  $RAO_S$ , the wave angles from  $0^\circ$  to  $180^\circ$  with an interval of  $30^\circ$  are considered due to the symmetry of the platform. The wave direction along the x-axis is  $0^\circ$ . The regular wave period ranges from 3 to 30 s with an interval of 0.2 s between 3 and 20 s and an interval of 2 s between 20 and 30 s.

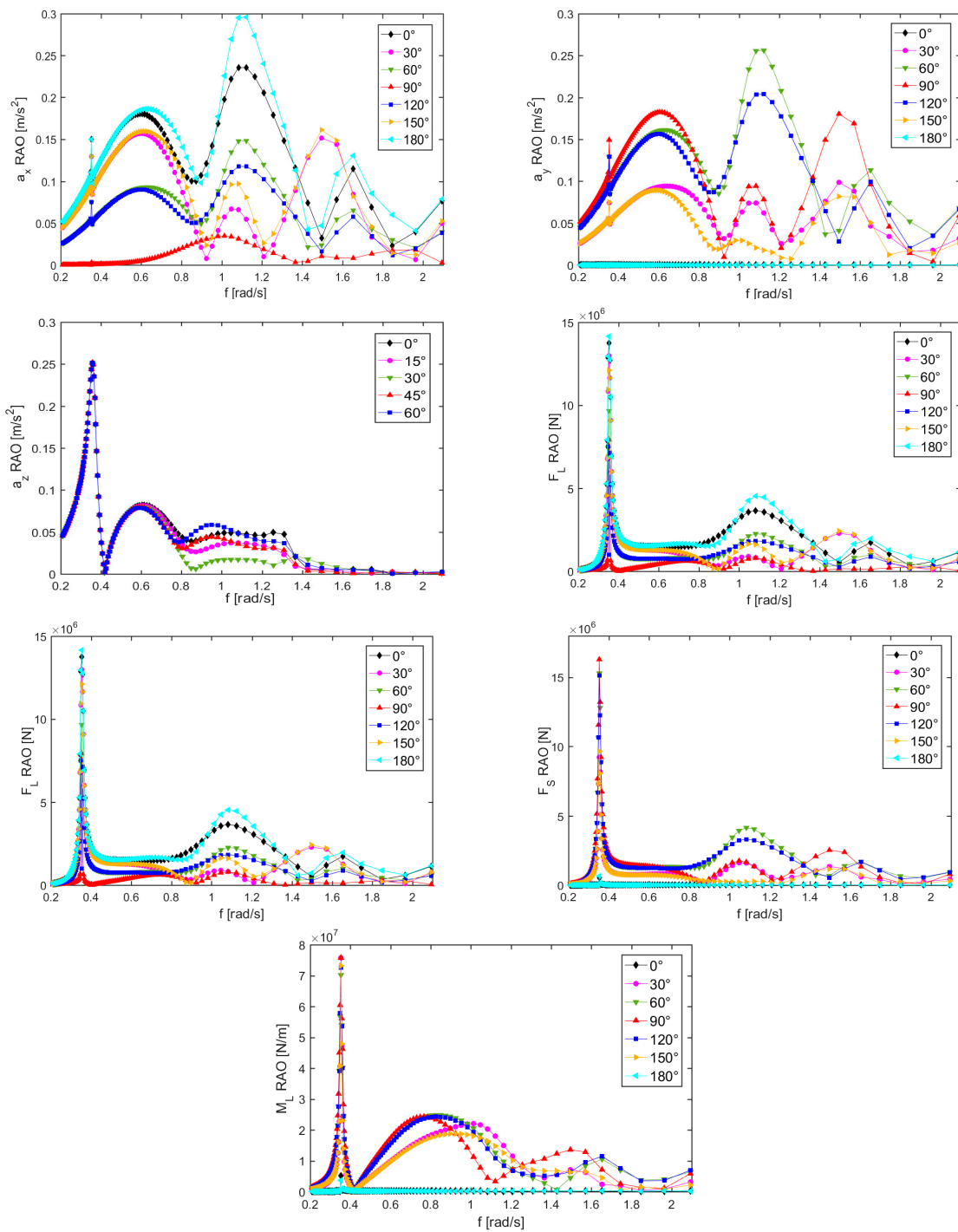


**Figure 8.** RAOs of various characteristic responses.

It can be seen from the figure that the peaks in the RAOs characteristic responses (except for  $a_x$  and  $a_y$ ) are located around 0.35 rad/s. The peaks occur in different wave directions. Local peaks also occur around 0.35 rad/s for the characteristic response of  $a_x$  and  $a_y$ , but the global peaks appear at other frequencies.

Based on the stochastic design wave method, the design wave parameters and the corresponding irregular wave parameters are listed in Table 3. The wave amplitude is calculated using Equation (3) with an  $LF$  of 1.3. The regular design waves are all obtained based on extreme wave conditions whose significant wave heights are close to the one for a return period of 100 years, i.e.,  $H_{s100}$ . It implies that the characteristic responses are monotonic to the wave conditions. For those extreme wave conditions, the possibility of the

occurrence of the wind speed below the cut-out wind speed is extremely low. The FOWT is in survival condition with parked turbines; thus, the wind load effects are insignificant. The waves mainly influence these characteristic responses. The use of the design wave method is reasonable. Design waves derived based on  $LF = 1.3$  are used in the following structural strength assessment to consider other effects the design wave method ignores.

**Table 3.** Design wave parameters and the corresponding irregular wave parameters.

Characteristic Response	Wave Direction	Wave Amplitude ( $LF = 1.3$ )	Period	Significant Wave Height	Spectral Peak Period
$a_x$	180°	7.78 m	5.6 s	14.03 m	16.07 s
$a_y$	90°	11.93 m	10.4 s	13.76 m	15.79 s
$a_z$	60°	7.75 m	17.6 s	14.15 m	16.64 s
$F_T$	90°	5.09 m	18 s	14.15 m	18.33 s
$F_L$	180°	4.92 m	17.8 s	14.15 m	18.33 s
$F_S$	90°	4.49 m	17.8 s	14.15 m	18.61 s
$M_L$	90°	4.53	17.8 s	14.15 m	18.05 s

#### 4.2. Extreme Load Effects Dominated by Wind Loads

According to the procedure of the modified ECM, the environmental condition that leads to the largest  $Mo_{X_{1-h},50}$  is  $H_s = 6.95$  m,  $T_p = 11.88$  s, and  $V = 24.8$  m/s, where  $V$  is the mean value wind speed at the height of the hub. The environmental condition is found in an environmental contour with a return period of 0.0119 years. The number of time-domain simulations for this environmental condition is 83, which satisfies the criterion proposed in [15]. The time history of the tower base  $F_x$  and  $M_y$  in one time-domain simulation is shown in Figure 9.

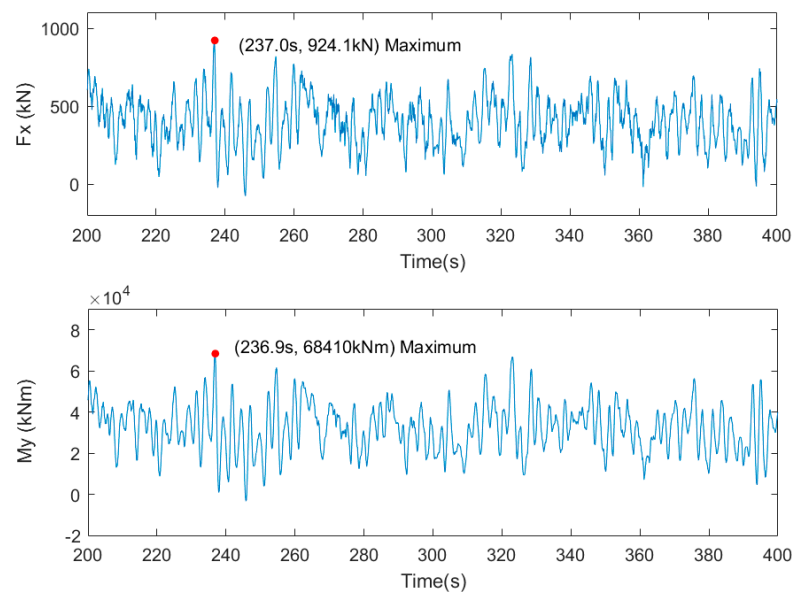


**Figure 9.** Time history of the tower base  $F_x$  and  $M_y$  in one time-domain simulation.

It can be seen that  $F_x$  and  $M_y$  are correlated and varied in a similar manner. The maximum  $F_x$  and  $M_y$  in the time histories occur almost simultaneously. The time difference between the two extreme values is 0.1 s, which is considered to be negligible.

The extreme values of the tower base  $F_x$  and  $M_y$  from all the simulations are used to regress the corresponding Gumble distribution based on the least square method. Figure 10 shows the data points and the regressed extreme value distributions.

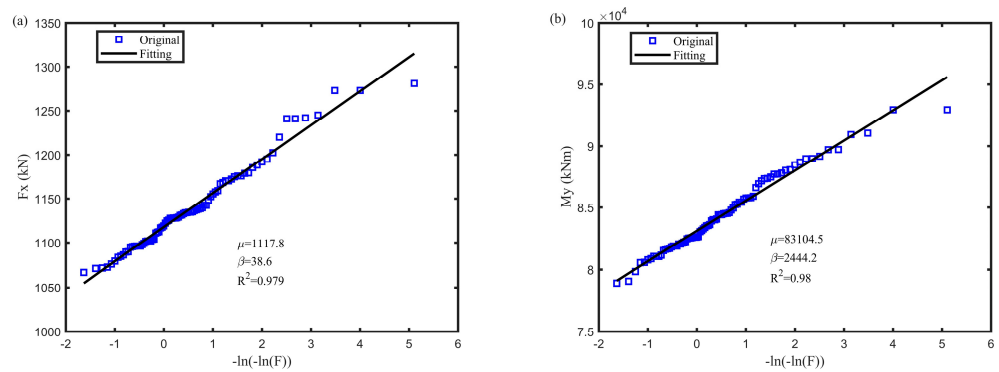


Figure 10. Gumbel distribution for the extreme tower base (a)  $F_x$  and (b)  $M_y$ .

The Gumbel distribution parameters  $\mu$  and  $\beta$ , and the coefficient of determination,  $R^2$ , which is a measure of the performance of data fitting, are also illustrated in the figure. The  $R^2$  values are close to 1, meaning the regression is quite reliable. The most probable extreme values extrapolated for the return period of 50 years are determined using Equation (13), and the results are  $F_x = 1.509 \times 10^3$  kN and  $M_y = 1.079 \times 10^5$  kN·m.

The extreme values of the tower base  $F_x$  and  $M_y$  are shown together in Figure 11. The correlation between the extreme  $F_x$  and  $M_y$  is also evident. The correlation coefficient is 0.91. It indicates that the extreme  $F_x$  and  $M_y$  can be approximated by a linear equation, as shown in Figure 11. If only the most probable extreme value of  $F_x$  for 50 years return period is obtained using Equation (13), the corresponding  $M_y$  can be approximated by the equation. The results are  $F_x = 1.509 \times 10^3$  kN and  $M_y = 1.079 \times 10^5$  kN·m. The  $M_y$  is underestimated by 2%.

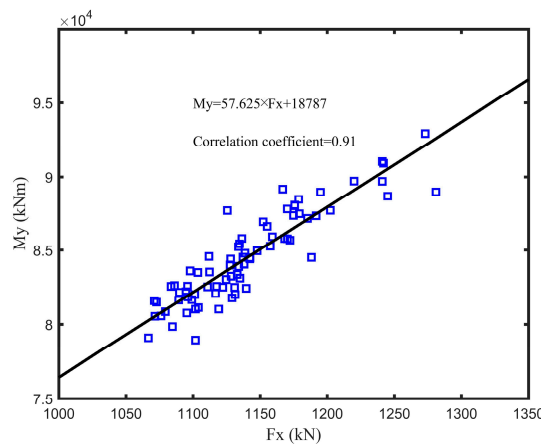


Figure 11. Correlation between the maximum tower base  $F_x$  and  $M_y$ .

In the present study, the most probable extreme values extrapolated for the return period of 50 years based on the two Gumbel distributions are applied to the finite element model. To illustrate the proposed method, the extreme values are only obtained when the wind direction is  $0^\circ$ . The effects of the wind direction on the load effects have been checked in some studies [10,11]. Their results indicate that the impact of wind direction on the extreme load effects of a 10 MW FOWT is insignificant. The effect is not clear for the FOWT investigated in the present study. The extreme values may vary significantly with direction. Further studies may be carried out to examine the effect of the wind direction on the extreme values of loads and the corresponding load effects.

#### 4.3. Finite Element Analysis Results

The maximum von Mises stress and its location for each load case are listed in Table 4. It can be seen that the maximum von Mises stress appears at different locations for different

load cases. The frame at the bottom of the outer column is the critical location for five load cases. The stress distribution in the frame for load case 7 is shown in Figure 12. The maximum stress is located at the toe of the bracket. The bracket toe is also the maximum stress location for the other four load cases. High stresses appear at several bracket toes. It indicates that the frame design is essential for structural strength. To reduce the maximum stress occurring at the bracket toe, the bracket may be replaced by a continuous web frame.

**Table 4.** Maximum von Mises stress and its location for each load case.

Load Case	Extreme Load Effects	Max. von Mises Stress (MPa)	Critical Location
1	$a_x$	291.8	Connection between outer column and diagonal brace
2	$a_y$	300.2	Frame in the bottom of outer column
3	$a_z$	296.4	Frame in the bottom of outer column
4	$F_T$	306.3	Frame in the bottom of outer column
5	$F_L$	319	Connection between centre column and upper horizontal brace
6	$F_S$	279.9	Frame in the bottom of outer column
7	$M_L$	320.5	Frame in the bottom of outer column
8	$F_x, M_y$	191.1	Connection between centre column and upper horizontal brace

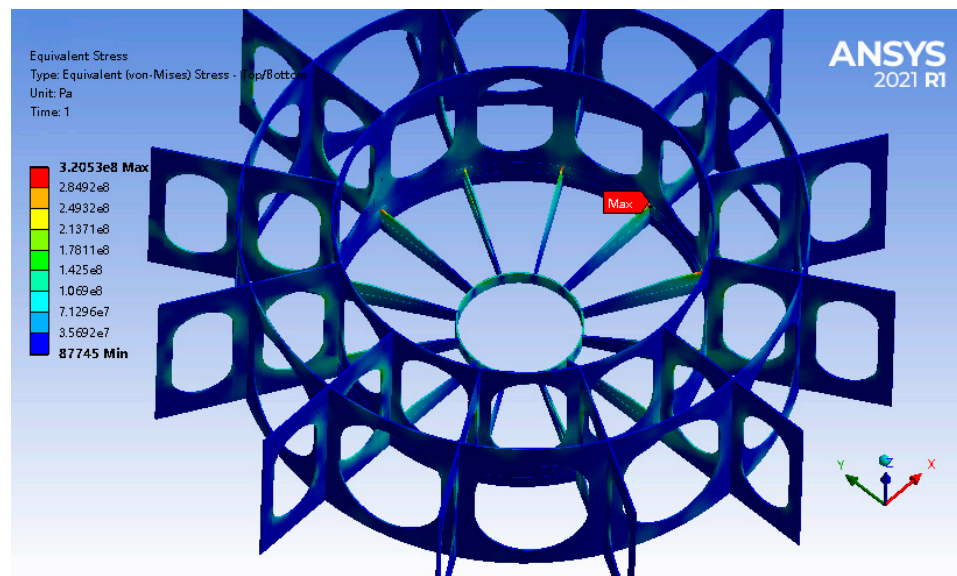


**Figure 12.** Stress distribution in the frame of bottom of outer column for load case 7.

The connection between the centre column and the upper horizontal brace is the critical location for two load cases, i.e., load cases 5 and 8. Figure 13 shows the stress distribution around the connection for load case 5. The high stress area is located at the column instead of the brace. It indicates that the wave load can also result in significant stress in the area close to the tower base. The stress is even higher than the stress of load case 8, where the extreme tower base forces and moment are applied. Only using the tower base load effects to evaluate the strength around the area may not be conservative. In addition, the fatigue strength of the highly stressed areas may be further checked.

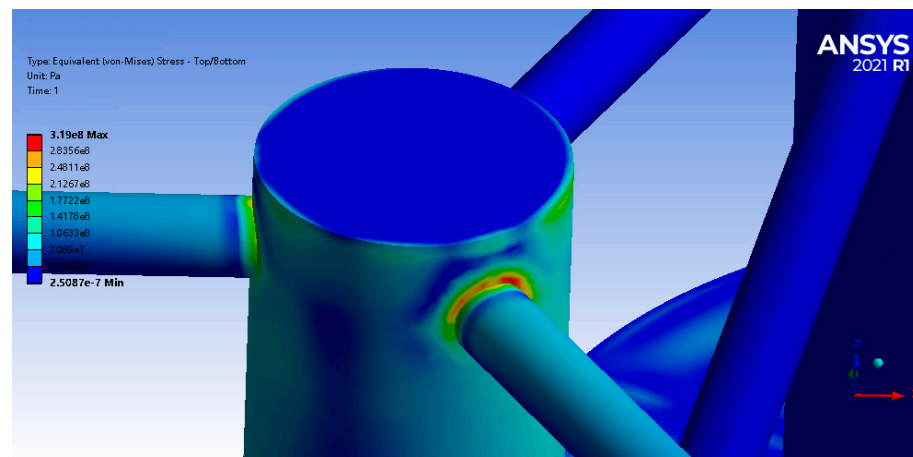


**Figure 13.** Stress distribution in the connection between the centre column and the upper horizontal brace for load case 5.

## 5. Conclusions

A simplified strength assessment method is developed for the preliminary structural design of an FOWT support structure to avoid difficulties in fully coupled load effects analyses and the large number of design load cases encountered in current practice. The method is developed based on the traditional design wave method and the modified ECM, including eight load cases involving limited time-domain simulations. The proposed method can be used in the preliminary design of similar FOWT support structures, in which the load cases can be altered based on the characteristics of the support structure. The following conclusions are established.

- Seven characteristic responses of the FOWT semi-submersible platform due to waves are chosen. The design waves for the extreme characteristic responses are all from extreme wave conditions where the significant wave heights are close to the one for a return period of 100 years. These characteristic responses are dominated by the wave loads.
- The short-term extreme values of the tower base shear force and bending moment conform to the Gumbel distribution. The maximum tower base shear force and bending moment have occurred almost simultaneously in the history of time. The extreme tower base shear force and bending moment values are correlated, and a linear equation can approximate the relationship between the two extreme values.
- For these load cases, the maximum stress appears at the frame of the outer column bottom, the connection between the centre column and the upper horizontal brace, and the connection between the outer column and diagonal brace. The frame design of the bottom of the outer column is essential for structural strength. The wave load can also result in significant stress in the area close to the tower base.

The effect of the wind direction on the extreme tower base forces and stresses can be further investigated. The simplified strength assessment method may be verified by comparing it with the method based on time-domain simulations in the future.

**Author Contributions:** Conceptualisation, Y.D. methodology, Y.D. and J.Z.; validation, J.Z.; formal analysis, J.Z. and S.Z.; investigation, J.Z. and S.Z.; writing—original draft preparation, Y.D.; writing—review and editing, Y.G. All authors have read and agreed to the published version of the manuscript.

**Funding:** The present study is supported by the National Natural Science Foundation of China (Grant No. 52101350).

**Institutional Review Board Statement:** Not applicable.

**Informed Consent Statement:** Not applicable.

**Data Availability Statement:** The data supporting this study's findings are available from the corresponding author upon reasonable request.

**Conflicts of Interest:** The authors declare no conflicts of interest.

## Nomenclature

$A_D$	design regular wave amplitude
$a_x, a_y, a_z$	the accelerations in three directions of the platform
CDF	the cumulative distribution function
CI	confidence interval
DLC	Design load case
ECM	Environmental Contour Method
FLAT	Full Long-Term Analysis
FORM	First order reliability method
FOWT	Floating offshore wind turbine
$F_T$	the split force between two outer columns
$F_L$	the split force between one outer column and the other two outer columns
$F_S$	the shear force between one outer column and the other two columns
$F_x$	the extreme tower base shear force
$F_X^{LT}(\xi)$	the long-term CDF of $\xi$
$F_{X S}^{ST}(\xi s)$	the short-term CDF of $\xi$
$F_{X_{1-h}}$	the 1 h extreme CDF
$F_{X_{10-min}}$	the 10 min extreme CDF
$F_{X_{1-h,50}}$	extrapolation of 50-year 1 h CDF
$f_S(s)$	the probability density function (PDF) of $s$
$f_{U_w, H_s, T_p}(u, h, t)$	Joint distribution of mean wind speed, significant wave height, and spectral peak period
$H_s$	significant wave height
IFORM	Inverse first order reliability method
$K_{xx}, K_{yy}, K_{zz}$	Radius of gyration
$M_L$	the torsion moment between one outer column and the other two columns
$M_y$	the extreme tower base bending moment
$Mo_{X_{1-h,50}}$	the most probable value of $F_{X_{1-h,50}}$
PDF	the probability density function
RAO	Response amplitude operator
RAOc	the peak RAO at the critical wave period
$R_{max}$	maximum response
$S_w(\omega)$	the wave energy spectrum
$S_R(\omega)$	the response spectrum
$S_S$	irregular sea steepness
$s$	a set of environmental parameters representing the short-term environmental condition
$T_z$	average zero up-crossing wave period
$T_a$	average response zero up-crossing period
$T_p$	spectral peak period
$U_w$	mean wind speed (10 m above the mean sea level)
$(u_N, h_N, t_N)$	the environmental condition on the $N$ -year environmental contour
$V(z)$	mean wind speed at $z$ m above the mean sea level
$X$	structural response
$\xi$	the extreme value of the response of $X$ in a period

## References

1. International Electrotechnical Commission. *Wind Energy Generation Systems—Part 3-2: Design Requirements for Floating Offshore Wind Turbines*; IEC 61400-3-2; International Electrotechnical Commission: Geneva, Switzerland, 2019.
2. DNVGL. *Floating Wind Turbine Structures*; DNVGL-ST-0119; DNVGL: Bærum, Norway, 2018.
3. Wang, S.; Moan, T.; Gao, Z. Methodology for global structural load effect analysis of the semi-submersible hull of floating wind turbines under still water, wind, and wave loads. *Mar. Struct.* **2023**, *91*, 103463. [[CrossRef](#)]



4. Li, J.; Bian, J.; Ma, Y.; Jiang, Y. Impact of typhoons on floating offshore wind turbines: A case study of typhoon Mangkhut. *J. Mar. Sci. Eng.* **2021**, *9*, 543. [[CrossRef](#)]
5. Zheng, T.; Chen, N.-Z. Time-domain fatigue assessment for blade root bolts of floating offshore wind turbine (FOWT). *Ocean Eng.* **2022**, *262*, 112201. [[CrossRef](#)]
6. Balli, E.; Zheng, Y. Pseudo-coupled approach to fatigue assessment for semi-submersible type floating offshore wind turbines. *Ocean Eng.* **2022**, *261*, 112119. [[CrossRef](#)]
7. Zhao, Z.; Wang, W.; Shi, W.; Qi, S.; Li, X. Effect of floating substructure flexibility of large-volume 10 MW offshore wind turbine semi-submersible platforms on dynamic response. *Ocean Eng.* **2022**, *259*, 111934. [[CrossRef](#)]
8. Zhong, W.; Zhang, X.; Wan, D. Hydrodynamic characteristics of a 15 MW semi-submersible floating offshore wind turbine in freak waves. *Ocean Eng.* **2023**, *283*, 115094. [[CrossRef](#)]
9. Luan, C.; Gao, Z.; Moan, T. Development and verification of a time-domain approach for determining forces and moments in structural components of floaters with an application to floating wind turbines. *Mar. Struct.* **2017**, *51*, 87–109. [[CrossRef](#)]
10. Wang, S.; Moan, T. Methodology of load effect analysis and ultimate limit state design of semi-submersible hulls of floating wind turbines: With a focus on floater column design. *Mar. Struct.* **2024**, *93*, 103526. [[CrossRef](#)]
11. Wang, S.; Moan, T. Analysis of extreme internal load effects in columns in a semi-submersible support structure for large floating wind turbines. *Ocean Eng.* **2024**, *291*, 116372. [[CrossRef](#)]
12. Park, S.; Choung, J. Structural Design of the Substructure of a 10 MW Floating Offshore Wind Turbine System Using Dominant Load Parameters. *J. Mar. Sci. Eng.* **2023**, *11*, 1048. [[CrossRef](#)]
13. Zavvar, E.; Abdelwahab, H.S.; Uzunoglu, E.; Chen, B.-Q.; Guedes Soares, C. Stress Distribution on the Preliminary Structural Design of the CENTEC-TLP under Still Water and Wave-Induced Loads. *J. Mar. Sci. Eng.* **2023**, *11*, 951. [[CrossRef](#)]
14. Zhang, J.; Dong, Y.; Garbatov, Y.; Li, H.; Chen, P. Design loads for strength assessment of floating offshore wind turbine semi-submersible platform. *Ships Offshore Struct.* **2024**. *submitted*.
15. Li, Q.; Gao, Z.; Moan, T. Modified environmental contour method for predicting long-term extreme responses of bottom-fixed offshore wind turbines. *Mar. Struct.* **2016**, *48*, 15–32. [[CrossRef](#)]
16. Barj, L.; Jonkman, J.M.; Robertson, A.; Stewart, G.M.; Lackner, M.A.; Haid, L.; Stewart, S.W. Wind/wave misalignment in the loads analysis of a floating offshore wind turbine. In Proceedings of the 32nd ASME Wind Energy Symposium, National Harbor, MD, USA, 13–17 January 2014; p. 0363.
17. DNVGL. *Column-Stabilised Units*; DNVGL-RP-C103; DNVGL: Bærum, Norway, 2015.
18. ABS. *Rules for Building and Classing Mobile Offshore Units—Part 3, Hull Construction and Equipment*; ABS: Houston, TX, USA, 2023.
19. Rosenblatt, M. Remarks on a multivariate transformation. *Ann. Math. Stat.* **1952**, *23*, 470–472. [[CrossRef](#)]
20. Winterstein, S.R.; Ude, T.C.; Cornell, C.A.; Bjerager, P.; Haver, S. Environmental parameters for extreme response: Inverse FORM with omission factors. In Proceedings of the ICOSSAR-93, Innsbruck, Austria, 9–13 August 1993; pp. 551–557.
21. Haver, S.; Kleiven, G. Environmental contour lines for design purposes: Why and when? In Proceedings of the International Conference on Offshore Mechanics and Arctic Engineering, Vancouver, BC, Canada, 20–25 June 2004; pp. 337–345.
22. Liu, J.; Thomas, E.; Goyal, A.; Manuel, L. Design loads for a large wind turbine supported by a semi-submersible floating platform. *Renew. Energy* **2019**, *138*, 923–936. [[CrossRef](#)]
23. Haselsteiner, A.F.; Frieling, M.; Mackay, E.; Sander, A.; Thoben, K.-D. Long-term extreme response of an offshore turbine: How accurate are contour-based estimates? *Renew. Energy* **2022**, *181*, 945–965. [[CrossRef](#)]
24. Robertson, A.; Jonkman, J.; Masciola, M.; Song, H.; Goupee, A.; Coulling, A.; Luan, C. *Definition of the Semi-Submersible Floating System for Phase II of OC4*; National Renewable Energy Lab. (NREL): Golden, CO, USA, 2014.
25. Zhu, X. Study on Response and Optimisation of Floating Offshore Wind Turbine under Extreme Sea Conditions. Master's Thesis, South China University of Technology, Shenzhen, China, 2020. (In Chinese).
26. Yang, Y.; Bashir, M.; Michailides, C.; Li, C.; Wang, J. Development and application of an aero-hydro-servo-elastic coupling framework for analysis of floating offshore wind turbines. *Renew. Energy* **2020**, *161*, 606–625. [[CrossRef](#)]
27. Li, L.; Gao, Z.; Moan, T. Joint distribution of environmental condition at five European offshore sites for design of combined wind and wave energy devices. *J. Offshore Mech. Arct. Eng.* **2015**, *137*, 031901. [[CrossRef](#)]

**Disclaimer/Publisher's Note:** The statements, opinions and data contained in all publications are solely those of the individual author(s) and contributor(s) and not of MDPI and/or the editor(s). MDPI and/or the editor(s) disclaim responsibility for any injury to people or property resulting from any ideas, methods, instructions or products referred to in the content.